Paper 05F-21 - Presented at the Fall 2005 Western States Section of the Combustion Institute, Stanford University, Oct. 17-18, 2005

Detailed and Simplified Chemical Reaction Mechanisms for Detonation Simulation

S. Browne, Z. Liang, and J. E. Shepherd
California Institute of Technology, Pasadena, CA 91106

October 13, 2005

Abstract

We examine the chemical basis for simplified chemical reaction models by using numerical simulations of adiabatic explosion with detailed chemical kinetic mechanisms under pressure and temperature conditions relevant to detonations. We have studied hydrogen, methane, and ethane to determine the reaction structure and characterize it in terms of three overall features: induction time, energy release pulse width, and reduced effective activation energy. A basic requirement of any realistic reaction model is that these three features should be reproduced over a range of conditions encountered within the detonation front. As part of this study, we have examined the question of the existence of a temperature cutoff, which has been proposed as the basis for formulating previous three-step models. We show that a definite cutoff temperature does not exist for any of the fuels we examine but there is a shift in the principle reaction pathway for the hydrogen-oxygen system in the vicinity of the extended second explosion limit. This shift in mechanism is associated with a peak in the reduced effective activation energy. A five-step reaction model is proposed to represent this shift in pathways, and with the appropriate choice of parameters, we show that the key features of the hydrogen-oxygen mechanism can be reproduced.

1 Introduction

Simplified chemical reaction mechanisms have been widely used in multi-dimensional, unsteady simulations for detonations. Substantial progress (Fickett and Davis, 1979) was made early on by focusing on the simplest model of a one-step irreversible reaction. In the last two decades, many different approaches have been taken to develop more realistic models that are still computationally efficient. Although it is possible to develop reduced models in the modern sense using quasi-steady state or manifold methods (Eckett, 2000, Varatharajan et al., 2005, Varatharajan and Williams, 2002a,b, 2001, Lu et al., 2003), there is still a substantial amount of effort on simplified modeling of a more ad hoc nature. These simple models are in some sense an elaboration of the one-step model, using a notional reaction scheme with multiple steps between a set of pseudo-species in order to mimic the chemical processes. It is with this type of simplified reaction modeling that the present paper is concerned.

We are specifically interested in examining the three and four-step reaction models (for example, Short and Quirk, 1997 and Liang and Bauwens, 2005) that include initiation, branching, and termination steps. These models are designed to imitate the key features of a realistic chemical reaction mechanism without the computational expense associated with time integration of a large set of species. The three and four-step models are viewed as being more realistic than the traditional one-step models and therefore able to more realistically represent phenomena such as initiation and quenching of reaction in unstable detonations.

The origins of all simplified models of combustion reactions for explosions can be traced back to the pioneering studies of Semenov (1935), who discovered the key roles of thermal feedback and branching-chain reactions in explosions and proposed separate models of each process. A unified model was developed by Gray and Yang (1965) to treat explosions due to simultaneous thermal and chain mechanisms. This became the basis for the three-step model (Dold and Kapila, 1991, Short and Quirk, 1997) which characterizes the extended second limit by a cross-over temperature where the chain-branching and chain-termination reaction rates are equal. A simplified view of the situation is that above this temperature, branching dominates, while below, termination will slow down and possibly quench the reaction.

The situation with realistic combustion chemistry is more subtle and although chain termination may alter the explosion time, peroxide chemistry may ultimately still enable an explosion to occur (Voevodesky and Soloukhin, 1965). Dold and Kapila compared the three-step model with traditional one-step models and concluded that the one-step model is not appropriate for simulating detonation initiation in systems governed by chain-branching explosions. Ng and Lee (2003) also investigated direct initiation with the three-step model and concluded, like Dold and Kapila, that the three-step model better captures chain-branching behavior. Recently, Liang and Bauwens (2005) have presented a four-step model that predicts all three classical explosion limits. The range of applicability of these simplified models to specific fuel-oxidizer systems is an area of active research.

The classical explosion limits occur at much lower temperatures than the post-shock conditions in detonations, and unlike detonations, diffusive processes over a long time scale are important for limits in vessel explosions. The classical theory of the second limit for vessel explosions (Lewis and von Elbe, 1961) is based on the idea that in high-temperature combustion chemistry involving H atoms there is competition between branching-chain reactions and chain-termination reactions which produce HO_2. The standard explanation (Lewis and von Elbe, 1961) for the second explosion limit observed in vessel explosions is that below the limit, termination reactions proceed more quickly than branching reactions and the explosion is quenched since the long-lived peroxide intermediates created by termination diffuse to the walls before they can react.

The connection between the second explosion limit and detonations was first attempted by Belles (1959) whose goal was to use this idea to explain the then-accepted values of detonation limits, which were 18.3% hydrogen in air for lean mixtures. However, Dove and Tribbeck (1970) showed that it was not possible to neglect the further reactions involving HO_2 and H_2O_2, an assumption that Belles had adopted from the classic second explosion limit model. Experiments by Tieszen et al. (1986) demonstrated that detonations can be established at hydrogen concentrations as low as 12.7%, far less than Belles' proposed "limit" value. Detailed chemical reaction kinetic simulations by Shepherd (1986) showed that even for very lean mixtures, the large amounts of HO_2 and H_2O_2 that were initially formed behind the shock front would ultimately decompose to OH and a branching-chain reaction would eventually occur. It is now also appreciated (Lee, 1984) that the phenomena of detonation limits is inextricably related to the physical size, particularly for the initiation process (Dorofeev et al., 2000). Based on these considerations, in the case of hydrogen-oxygen detonations, the existence of the second explosion limit and competition for radicals does not appear to directly result in intrinsic limits for the existence of detonations in the simple manner that Belles proposed. The situation for hydrocarbon fuels is less clear. Although low-temperature explosion limits are observed for hydrocarbon fuels, there has been relatively little exploration of the relevance of radical competition at higher temperatures to the problem of intrinsic detonation limits. One of the goals of the present study is to examine some representative hydrocarbon fuels with this aspect in mind.

The competition for H atoms in hydrogen combustion does appear to have an influence on detonation properties although in more subtle fashion than proposed by Belles. Strehlow and Cohen (1962) first noted that detonations initiated by reflected shock waves do not all exhibit similar character. Instead, there exist three categories which they define according to the process that accelerates the reflected wave. In the first category, the chemical reaction zone releases a weak pressure wave that accelerates the reflected wave. In the second category, the pressure wave becomes a shock wave before it interacts with the reflected wave. The third category discussed is unsteady and the authors propose that in this case a

very large amount of heat is released very quickly and the system remains unsteady until a detonation forms. These ignition regimes apparently reflect some underlying essential differences in the reaction mechanisms.

Voevodesky and Soloukhin (1965) found that a key factor in determining these ignition regimes was the role of an "extended second limit" between a fully-branched mechanism and a straight-chain mechanism with rare branching. They described two detonation initiation regimes divided by this limit and characterized qualitatively by schlieren streak photographs. 'Strong' initiation occurs at high temperatures and exhibits a single ignition locus. For lower temperatures, 'weak' initiation characterized by many loci which merge to form a single front dominates. They presented a theoretical limiting curve that was later re-evaluated by Gardiner and Wakefield (1970) who explored how changes in temperature translate to changes in kinetics. Meyer and Oppenheim (1970) further developed the concept of 'weak' and 'strong' initiation by deriving an alternate expression for the extended second limit and eventually presenting a coherence theory for ignition (Meyer and Oppenheim, 1971). They reasoned that distinct exothermic centers lead to the nonuniform nature of 'weak' initiation. Borisov (1974) investigated four origins of these exothermic centers: fluctuations in temperature, fluctuations in activated molecules, nonuniform heating due to wave interaction, and catalytic generation. Later, Oran and Boris (1982) examined the sensitivity of H_2-O_2 mixtures to sound waves and perturbations in entropy by superimposing the extended second limit on contours of induction time derivatives and comparing behavior on either side of the limit. They concluded that chemical competition between branching and termination reactions is the primary contributor to the shape of the sensitivity contours.

The nature of the chemical reaction model and the shape of the reaction zone structure also have a clear influence on the detonation stability. The existence of multiple length scales in the reaction zone and the relevance to experimental measurements of detonation cell width and cellular regularity was examined by Strehlow and Engel (1969). The difficulties with one-step models in numerical simulations and early work by Fickett et al. (1972) on branching-chain models motivated Short and Quirk (1997) and Short and Sharpe (2003) to investigate stability limits for three and two-step reactions. They concluded that detonation instability is strongly dependent on the ratio of the lengths of the induction zone and energy release zone. Increasing the length of the energy release zone relative to the induction zone stabilized the detonation. In the case of the three-step reaction proposed by Short and Quirk, this length ratio is governed by the value of the post-shock temperature relative to the cross-over temperature.

The shape of the reaction zone has a strong influence on initiation and stability. Ng and Lee (2003) used the same model as Short and Quirk to study detonation initiation, and they emphasized the importance of independently varying the ratio of energy release time to induction time as well as the activation energy. One-dimensional pulsating detonation simulations with detailed chemistry (Yungster and Radhakrishnan, 2005, 2004) for ethylene and hydrogen-air mixtures show a transition from high to low frequency modes with increasing equivalence ratio. This transition is associated with the changing shape of the reaction zone. Similar computations have been carried out by Ng et al. (2005) for the hydrogen-air system. Ng et al. found that the reaction zone shape, characterized by the ratio of induction length to energy release length, was important in developing predictive correlations for detonation cell width as well as the one-dimensional stability threshold. These studies all indicate that the ability to independently specify the induction and energy release times, as well as the effective activation energies, is an important aspect of any realistic chemical reaction model.

One of the key issues that arises in the three-step model used by Short and Quirk and also Ng and Lee is the interpretation of the cross-over temperature. Short and Quirk state: "If the detonation shock temperature drops to the chain-branching cross-over temperature T_B, the detonability limit occurs." Ng and Lee state: "For successful initiation, the blast wave generated by the source must not drop below the chain-branching cross-over temperature before the onset of detonation occurs." However, the experimental studies cited previously all indicate that chemical reaction does not cease and detonations can be initiated at and below the extended second limit. The previous work does show that there are definite changes in the detonation behavior and shifts in the chemical pathways at the extended second limit for H_2-O_2. However, there is no reason to believe that chemical reaction stops below a definite cross-over temperature, and even the existence of a cross-over effect has not been generalized to fuels

other than hydrogen.

In order to clarify the situation with regard to the reaction zone parameters and the cross-over temperature, we have carried out numerical simulations of constant volume explosions based on realistic reaction mechanisms and rates for selected fuels (H_2, CH_4, C_2H_6) and diluents (N_2, Ar). We examine three overall features of the reaction zone: the induction time, energy release time, and effective activation energy. While the specific reaction paths involved for different chemical mixtures can vary dramatically, these overall features give a set of parameters that can be compared with those of reduced mechanisms. We begin by presenting the constant volume explosion model and discuss the determination of the overall parameters in Section 2. Then we present simulation results for a variety of mixtures in Section 3. The structure of the reaction zone and dependence of the parameters on temperature is analyzed for the existence of a cross-over temperature. The variation of the parameters within an unstable detonation is considered. In Section 4, we propose and discuss preliminary results of a five-step model that reproduces some key features of the hydrogen-oxygen reaction zones.

2 Detonation Reaction Zone Modeling

Propagating detonations are unsteady and spatially nonuniform. For the present purposes, it is necessary to adopt a greatly simplified model of the physical processes in order to examine the chemical aspects in some detail. For steady detonations traveling at the Chapman-Jouguet (CJ) speed or higher (over-driven waves), it is possible to use the Zeldovich-von Neumann-Döring (ZND) model (Fickett and Davis, 1979). However, we would like to examine a wide range of temperatures and pressures, including the states accessed in unstable propagating waves, and the ZND model is too restrictive. Instead, we will use the conceptually simpler constant-volume (CV) explosion simulation. This is a zero-dimensional model that assumes the reactions take place at constant specific volume and internal energy. We assume initial conditions that are representative of the post-shock states in detonation waves.

The CV simulation (Browne and Shepherd, 2005) used in the present study was implemented in Matlab with realistic thermochemistry and a detailed chemical reaction mechanism. The chemical portion of the simulation is based on the the Cantera library (Goodwin, 2005), and a stiff ordinary differential equation solver is used to march in time from a specified initial state to near-equilibrium conditions. The program allows the user to specify the pre-shock or post-shock pressure, temperature, species mole fractions, and the shock speed. The program output consists of temporal profiles of the species amounts and the thermodynamic states.

In high-temperature, shock-induced combustion, the temporal evolution of the species usually consists of an induction period that is almost thermally neutral followed by an exothermic recombination period, Fig. 1. The induction time, τ, is determined by the location of maximum temperature gradient while the energy release pulse width, δ, is measured by the full-width at half-maximum locations. Figure 1 and all subsequent figures were created with the GRI mechanism with high temperature fits to the thermochemistry since the original data were not valid for all species up to 6000 K.

Figure 2 depicts how the induction time τ, and the energy release pulse width δ, vary in the post-shock temperature-pressure plane. From Fig. 2, τ depends primarily on temperature while δ depends primarily on pressure. The temperature sensitivity of the induction time is conventionally characterized by an effective activation energy, E_a, which can be obtained from an Arrhenius plot ($\ln(\tau)$ versus $1/T$). For a one-step model or an elementary reaction with a single activation energy, the result is

$$\ln(\tau) = \frac{E_a}{\mathcal{R}} \frac{1}{T} + \text{constant} \tag{1}$$

For a multi-step model, $E_a/\mathcal{R}$ can be defined as the local slope of the Arrhenius curve as depicted in Fig. 3a for a range of post-shock states in stoichiometric H_2-Air. The larger the activation energy, the more sensitive the induction time will be to fluctuations in temperature within the reaction zone. Stability computations and experimental studies of detonation structure (Austin et al., 2005) have shown that the reduced effective activation energy, $\theta = E_a/(\mathcal{R}T)$, where $\mathcal{R}$ is the ideal gas constant and T is

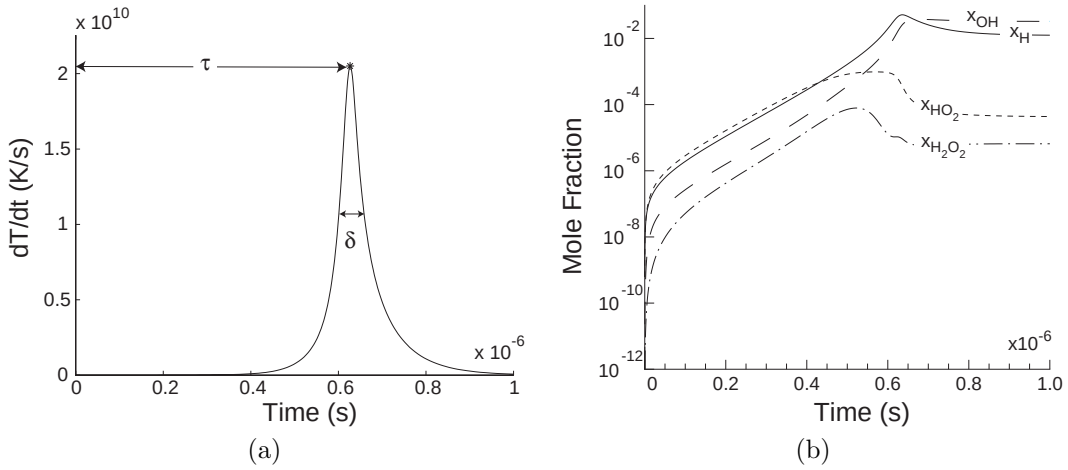

Figure 1: Constant-volume explosion in stoichiometric hydrogen-air, postshock conditions for CJ detonation, preshock conditions of 1 atm and 300 K. (a) Defintion of induction time, $\tau = 6 \cdot 10^{-7}$ s, and pulse width, $\delta = 6 \cdot 10^{-8}$ s. (b) Profiles of minor species.

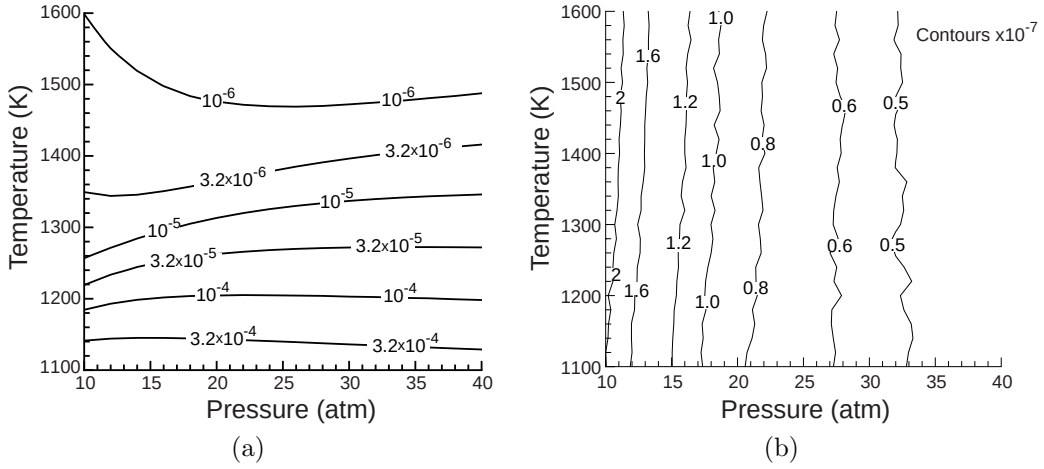

Figure 2: Pressure and temperature dependence of (a) τ, induction time, and (b) δ, energy release pulse width, simulated using CV explosion calculations with detailed chemistry for stoichiometric H_2-Air.

the post-shock temperature, is a figure of merit for judging stability. The larger the value of θ, the more irregular the cellular structure. More recently, Ng et al. (2005) have proposed that multiplying θ by a parameter proportional to τ/δ provides a better figure of merit for this purpose. For multi-step kinetics, the effective activation energy can be determined by numerically differentiating the curve in Arrhenius ordinates

$$\theta = \frac{1}{T_s} \frac{\ln(\tau_+) - \ln(\tau_-)}{\frac{1}{T_+} - \frac{1}{T_-}} \tag{2}$$

Here T_+ and T_- bracket T_s, i.e. $T_\pm = T_s \times (1 \pm 0.01)$, and τ_+ and τ_- are the corresponding induction times. The reliability of this technique and the choice of the amount of perturbation in temperature (1%) are discussed by Schultz and Shepherd (2000) and also Pintgen and Shepherd (2003). For hydrogen-oxygen mixtures, contours of θ in the post-shock temperature-pressure plane (Fig. 3b) exhibit a unique "ridge" of high activation energy which we will discuss in detail in the next section.

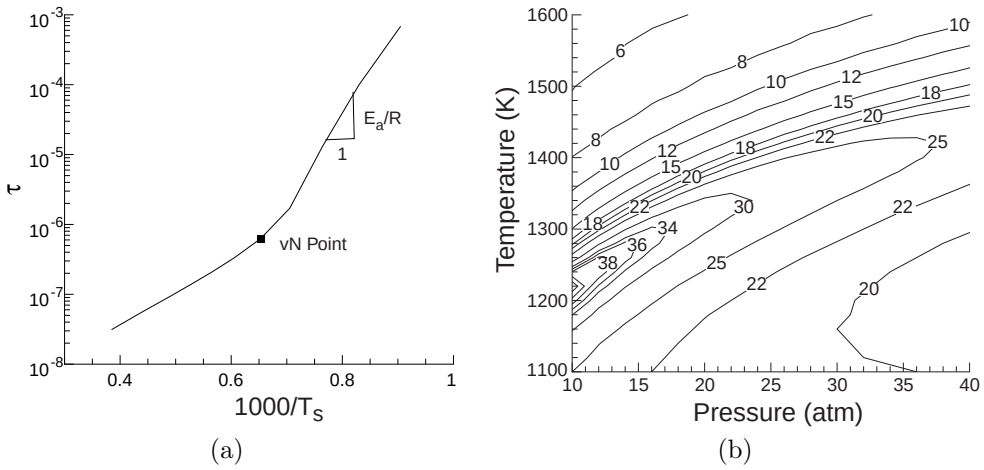

(a) (b)

Figure 3: (a) Arrhenius plot of induction time for a range of post-shock states in stoichiometric H_2-Air initially at standard conditions. The determination of $E_a/\mathcal{R}$ as the slope is shown. The point labeled vN is the von Neumann point, corresponding to the post-shock for a shock wave traveling at the CJ speed. (b) Reduced effective activation energy, θ, contour plot for stoichiometric H_2-Air mixtures.

3 Results

In this section, we show the results of computations using detailed chemistry for three fuels: H_2, CH_4 and C_2H_6. In all three cases, the reaction mechanism and rates of the GRI mechanism for natural gas have been used. There are many combinations of initial conditions possible for these simulations and we have focused on a few relevant to ambient conditions with air as the oxidizer. Experiments using argon dilution are also commonly carried out with hydrogen-oxygen mixtures at reduced pressure in the laboratory so some results for these are also included.

3.1 Hydrogen

Minor species temporal histories for representative cases are shown in Figs. 1 and 4. These illustrate the well-known features of high-temperature H_2 oxidation. The ignition process begins with an initiation step,

$$H_2 + O_2 \rightarrow HO_2 + H, \tag{R1}$$

which creates a small amount of radicals. Following the generation of the initial seed amounts of HO_2 and H, one of two pathways are followed. At high temperature and low pressure, the dominant initial process is chain branching

$$H + O_2 \rightleftharpoons OH + O, \tag{R2}$$
$$O + H_2 \rightleftharpoons OH + H, \tag{R3}$$
$$OH + H_2 \rightleftharpoons H_2O + H, \tag{R4}$$

which results in exponential growth of H, O, and OH. At low temperature and high pressure, the dominant initial process is through the so-called "chain-termination" reaction

$$H + O_2 + M \rightleftharpoons HO_2 + M. \tag{R5}$$

In vessel explosions at low temperatures (300-400°C), the HO_2 is sufficiently nonreactive that the radicals diffusive to the walls before the further reaction takes place and the explosion process is indeed

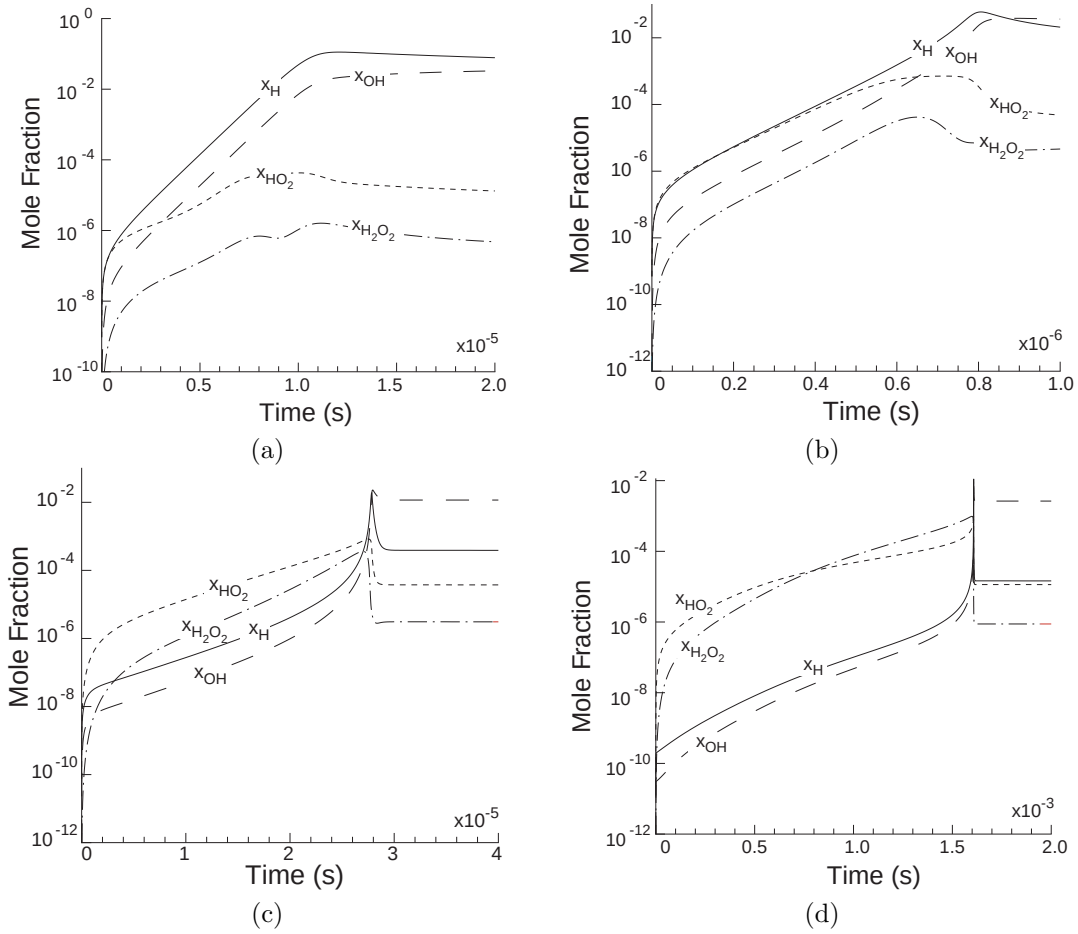

Figure 4: Minor species profiles for constant volume explosions in H_2-air mixtures at various conditions. (a) $\phi = 1$, post-shock pressure of 1 atm and temperature of 1550 K. (b) $\phi = 1$, pre-shock pressure of 0.7 atm and temperature of 300 K, CJ shock speed. (c) $\phi = 0.5$, pre-shock pressure of 0.7 atm and temperature of 300 K, CJ shock speed. (d) $\phi = 0.35$, pre-shock pressure of 0.7 atm and temperature of 300 K, CJ shock speed.

terminated. In detonations, the temperature is still sufficiently high ($> 900°C$) that the HO_2 reacts through either

$$HO_2 + H \rightleftharpoons OH + OH, \tag{R6}$$

or

$$HO_2 + HO_2 \rightarrow H_2O_2 + O_2, \tag{R7}$$

$$H_2O_2 + M \rightleftharpoons OH + OH + M. \tag{R8}$$

After a sufficient quantity of OH radicals have been produced through this "straight-chain", the chain-branching process will take over and exponential growth of H, O, and OH takes places. In either case, near the end of the branching-chain process, the main energy release occurs through the recombination reaction,

$$H + OH + M \rightleftharpoons H_2O + M. \tag{R9}$$

Reaction	A	n	E_a
R2. $H + O_2 \rightarrow OH + O$	$2.65 \cdot 10^{16}$	-0.67	17041
R5. $H + O_2 + M \rightarrow HO_2 + M$	$2.8 \cdot 10^{18}$	-0.86	0
R8r. $OH + OH + M \leftrightarrow H_2O_2 + M$	$2.3 \cdot 10^{18}$	-0.90	-1700

Table 1: Partial Hydrogen Oxidation Mechanism and Rate Constants taken from the GRI mechanism

The reaction rate coefficients for all of these reactions are given in the modified Arrhenius form,

$$k = AT^n \exp\left(\frac{-E_a}{\mathcal{R}T}\right) . \tag{3}$$

In the case of the three-body reactions, transition from low-pressure to high-pressure forms of the rate constant are specified. For the present purposes, although we consider elevated pressures in comparison to usual laboratory vessel explosions, the pressures are still sufficiently low that the low-pressure form of the rate constants can be used. Rate coefficients for a few of the relevant reactions in the H_2-O_2 mechanism are given in Table 1.[1]

R2 is the rate-limiting reaction for chain-branching sub-mechanism and R8 is the rate-limiting reaction for the straight-chain sub-mechanism. These two reactions determine the effective activation energy for the overall reaction in the respective regimes. The competition between these two sub-mechanisms is determined by the trade-off between reactions R2 and R5. Considering the form of the modified Arrhenius rate (3), R2 is strongly sensitive to temperature with an activation energy of about 17 kcal/mol while R5 has zero activation energy and is, by comparison, temperature insensitive. In addition, R2 is bimolecular, while R5 is trimolecular so that the relative importance of R5 will increase with increasing pressure. Reaction R8 is also strongly temperature sensitive with an activation energy of about 44 kcal/mole.

The simple picture is that during the induction period (Section 2), characterized by τ, the bimolecular chain-branching reactions produce the pool of radicals and then during the exothermic recombination period, characterized by δ, trimolecular reactions such as R5 and R9 recombine radicals into products. Therefore, as shown in Fig. 2, τ depends mainly on temperature and δ depends mainly on pressure. The ratio, τ/δ, relating the length scales of the induction zone and the energy release zone is a nondimensional parameter characterizing the mixture that should be matched by a reduced mechanism. Because the temperature dependence of τ is stronger than the pressure dependence of δ, contours of this ratio shown in Fig 5a are similar to contours of τ. The change in pathways between the two sub-mechanisms results in a change in slope in the Arrhenius plots of Fig. 5b. The lower slope seen at high temperatures and in the low pressure case corresponds approximately to the value of activation energy for R2 while that larger slope observed at low temperature for the high pressure cases corresponds to the value for R8. The larger intermediate slopes are what give rise to the ridge of high normalized activation energy visible in Fig. 2. The difference in pressure dependence of reactions R2 and R5 results in different scaling for the induction time and energy release time. At low pressures and low temperatures, Fig. 5c, $\tau \sim P^{-1}$ and $\delta \sim P^{-2}$. The change in slope of τ between 10 and 40 atm is connected with the change in sub-mechanism. At high temperatures, Fig. 5d, the slopes are slightly smaller in magnitude and there is only a slight variation in the slope of τ since these states are well away from the cross-over region.

Examination of the species plots shows that while this simple picture is correct for laboratory experiments carried out at low initial pressures (0.1 atm), Fig. 4a, the situation is more complex for the cases shown in Figs. 4b,c,d. The latter are more typical of accidental explosions or field testing, which take place at 1 atm or above. For the higher initial pressures, HO_2 is always present in substantial amounts and the H atoms and the chain-branching process dominate only near the very end of the induction zone. In Fig. 4d, the mixture composition is completely dominated by HO_2 and H_2O_2 in the initial stages, which in the classical view of the extended second limit is a mixture that could not detonate. In fact, mixtures at this equivalence ratio have been detonated by Tieszen et al. (1986).

[1] Units are centimeters, seconds, Kelvin, and calories/mole

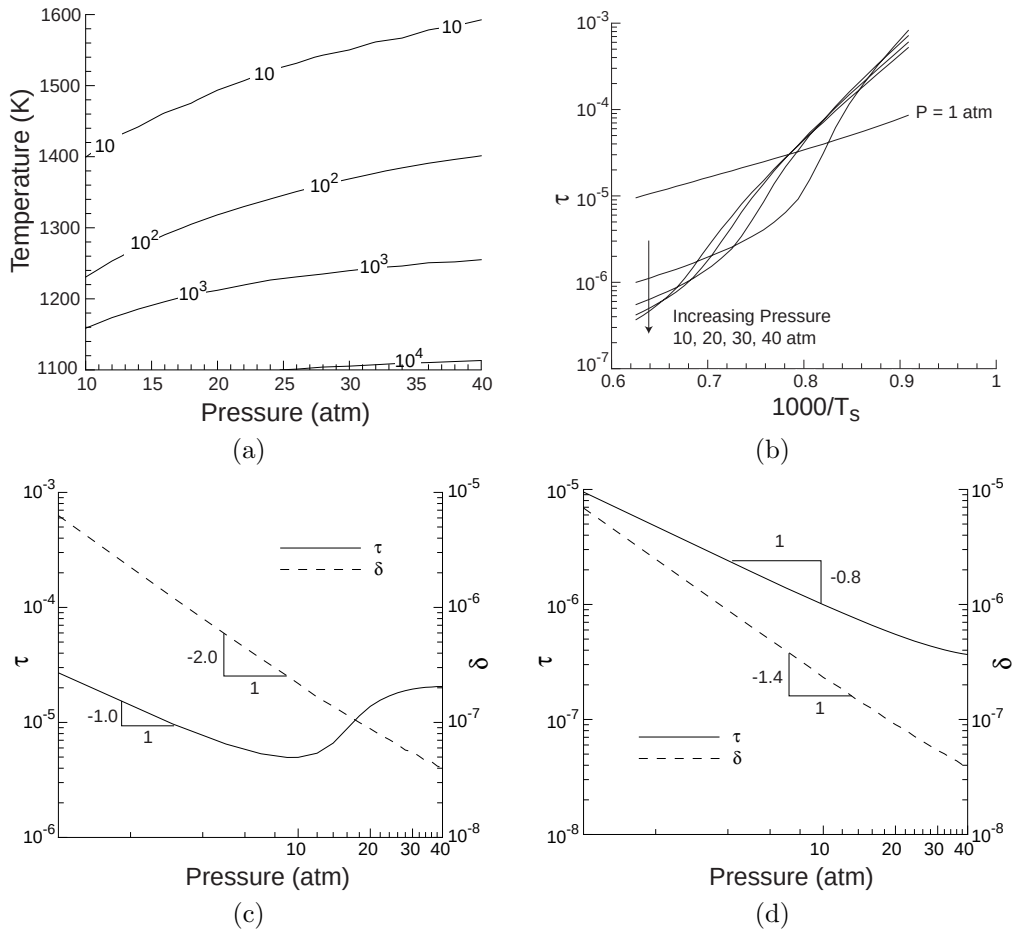

Figure 5: Stoichiometric H_2-air mixtures. (a) Contours of constant τ/δ (b) Induction time versus temperature in Arrhenius coordinates. (c) Pressure scaling of induction time and energy release time with pressure at 1300 K. (d) Pressure scaling of induction time and energy release time with pressure at 1600 K.

In early discussions of the competition between the chain branching and termination (Voevodesky and Soloukhin, 1965), the temperature-pressure plane was divided into two sections separated by a single curve setting the ratio of reaction rates for reactions R2 and R5 to a specified value of order one. This is apparently one of the origins of the notion of cross-over temperature that is used in the three-step models. However, it is clear from the plots of the species and the reduced effective activation energy, θ, that the competition occurs over a wide range of temperatures, depending on the pressure. This is indicated by the broad "ridge" of high values of θ seen in Fig. 2. This ridge is unique to the H_2-O_2 system but occurs for a wide range of mixtures (air, oxygen, oxygen diluted with argon) and equivalence ratios. Figure 6 illustrates the effects of (a) argon dilution and (b) equivalence ratio on the contours of effective activation energy. While the location of the ridge is slightly shifted amongst these mixtures, its presence is visible in all hydrogen mixtures we examined, indicating that the competition region appears to be generic to hydrogen.

These simulations make it clear than only in very specific cases (low pressure and high temperature) is it possible to clearly separate chain branching of H, O, and OH from the straight-chain reactions involving HO_2 and H_2O_2. For most cases, the two mechanisms proceed simultaneously. In addition, the so-called extended second limit is really a broad transition zone between the two mechanisms and does

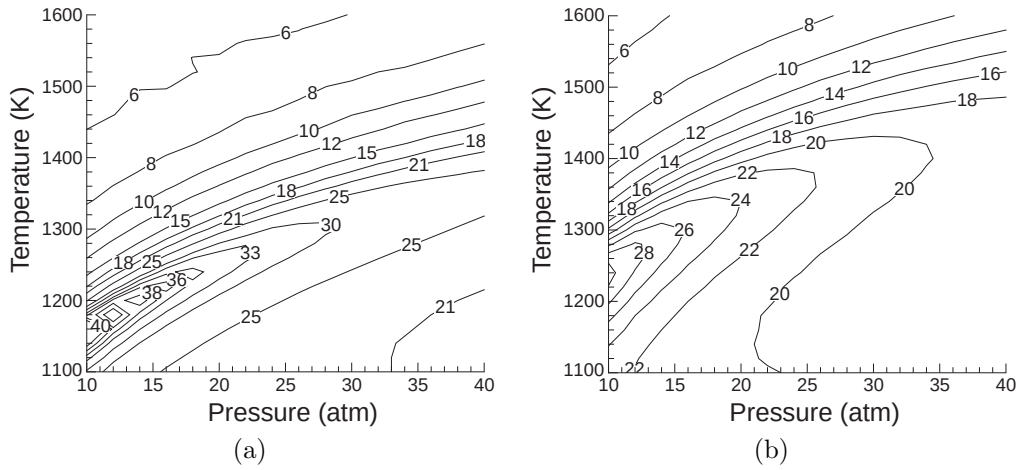

Figure 6: Contours of constant θ for (a) stoichiometric H_2-O_2 with 85% argon dilution and (b) rich H_2-O_2 ($\phi = 3.0$).

not represent any sort of a limit to reaction progress as detonations are observed to occur on both sides of this zone. The real significance of the extended second limit is that it appears to mark the "ridge line" of the transition process and indicates where the maximum values of reduced activation energy will be found.

3.2 Methane

Results for one mixture are shown in Fig. 7. Induction times and activation energies are a monotonic and smoothly varying function of pressure, indicating that for this mixture, there is no cross-over effect.

3.3 Ethane

CV computations for stoichiometric ethane-air are shown in Fig. 8. The results are very similar to methane and there is no evidence of a cross-over effect in any of these plots.

3.4 Detonation Conditions

A wide range of thermodynamic conditions are relevant to detonation simulation because in a multidimensional detonation, the shock front oscillates substantially in amplitude. Simulations based on simplified mechanisms and estimates from laboratory experiments suggest that a typical range for shock front velocities is $0.8U_{CJ}$ to $1.4U_{CJ}$. From the shock jump conditions and this variation in velocity, the corresponding range of states in the temperature-pressure plane can be computed. This range is shown superimposed on the θ contours in Fig. 9a. The three distinct points on each curve indicate post-shock states corresponding to different overdrive values where the lowest point is for an underdriven wave, $0.8U_{CJ}$, and the highest point is for an overdriven wave, $1.2U_{CJ}$. As the shock speed decreases, it is possible that the post-shock state crosses into the competition region and the reduced effective activation energy increases. A similar effect occurs when comparing the von Neumann points of mixtures with varying equivalence ratios as shown in Fig. 9b. Like the curves in Fig. 9a, lower initial pressures shift the curve to the left and cause the system to interact more with the competition region. Inspection of minor species profiles confirms the transition from production of H atoms to production of peroxide (H_2O_2). This effect will almost certainly be important for detonation stability analysis in this regime.

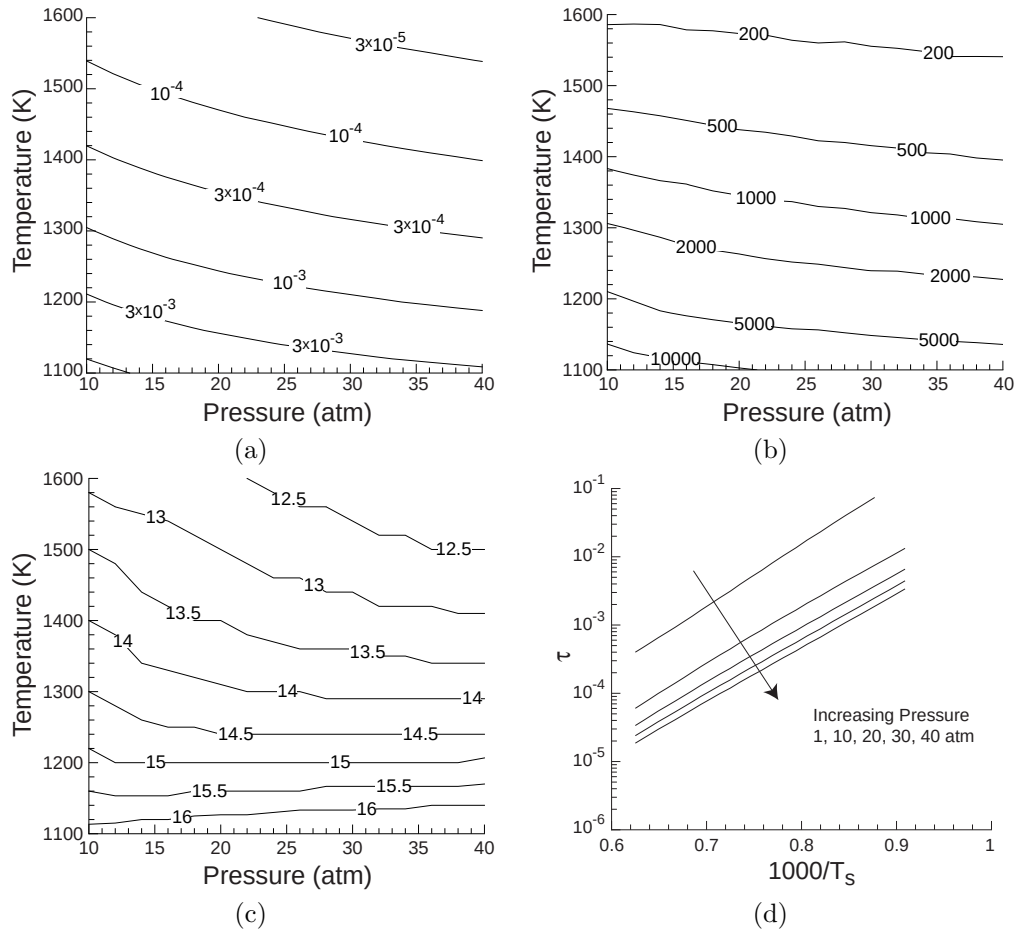

Figure 7: Constant volume explosion calculations with detailed chemistry for stoichiometric CH_4-O_2 (a) induction time τ, (b) ratio of induction time to energy release time (τ/δ) (c) normalized effective activation energy θ, (d) temperature dependence of the induction time for five pressures.

4 Five-step hydrogen-oxygen model

Based on the results of the chemical reaction kinetics simulations discussed above, we conclude a new type of simplified model is required to reproduce the reaction zone features that we observe in the hydrogen-oxygen system near the extended second limit. In particular, we would like to reproduce the two pathways for oxidation: the branching chain for H atoms, and the straight-chain production of HO_2 and H_2O_2. The model should be able to mimic the competition between these processes, the resulting induction times, energy release time, and effective activation energy dependence on temperature and pressure.

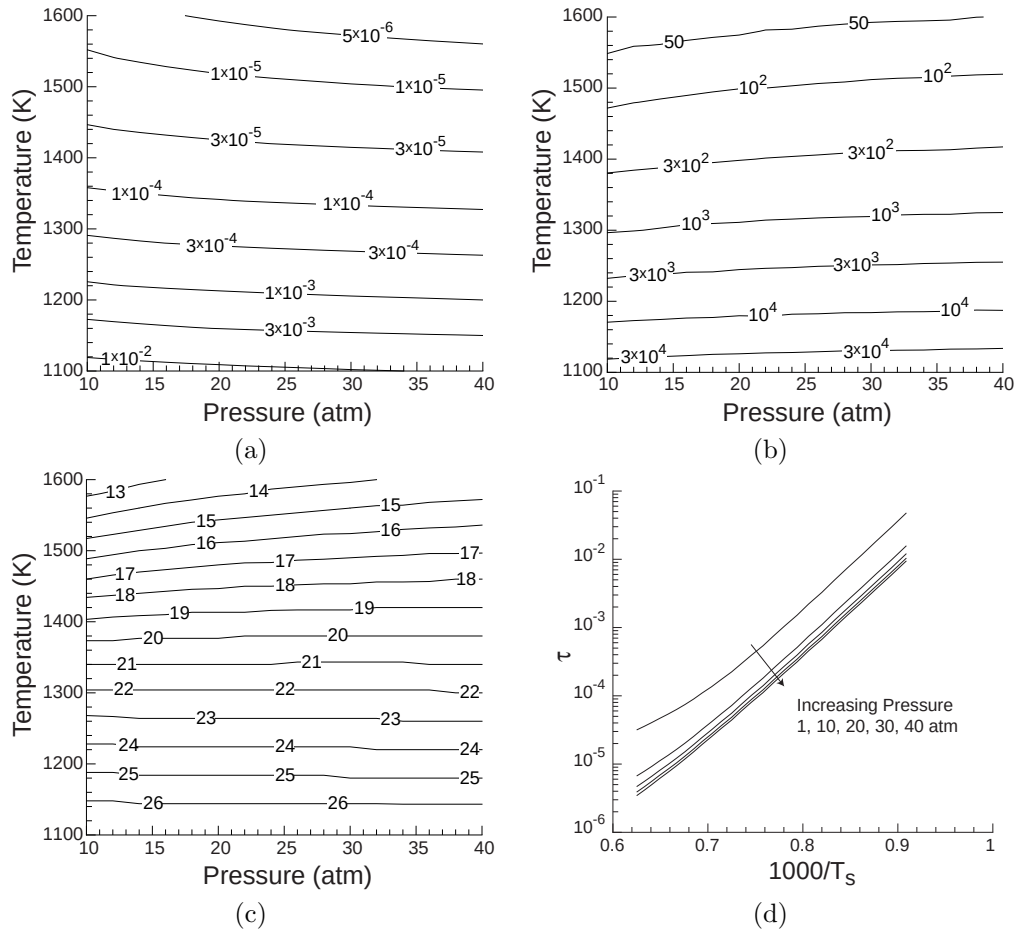

Figure 8: Constant volume explosion calculations with detailed chemistry for stoichiometric C_2H_6-O_2 (a) induction time τ, (b) ratio of induction time to energy release time (τ/δ) (c) normalized effective activation energy θ, (d) temperature dependence of the induction time for five pressures.

Our proposed scheme is,

$$R \overset{k_1}{\rightarrow} B \tag{S1}$$

$$R + B \overset{k_2}{\rightarrow} 2B \tag{S2}$$

$$R + B + M \overset{k_3}{\rightarrow} C + M \tag{S3}$$

$$C \overset{k_4}{\rightarrow} B \tag{S4}$$

$$B + B + M \overset{k_5}{\rightarrow} P + M \tag{S5}$$

where R represents the pseudo reactants (H_2 or O_2), B is the chain radical (H, O, or OH), C is the intermediate species (HO_2 or H_2O_2), P is the product (H_2O), and M is a chaperon molecule. S1, S2, and S4 are temperature dependent while S3 and S5 are temperature independent but pressure dependent. Heat release is only associated with the termination step, S5. Here S2 and S3 represent elementary steps competing for H atoms in the actual H_2-O_2 chemistry. A modified Arrhenius rate constant formulation was used for all steps and the parameters were chosen by analogy to the actual rate constants used in the GRI mechanism, with some adjustment by trial and error.

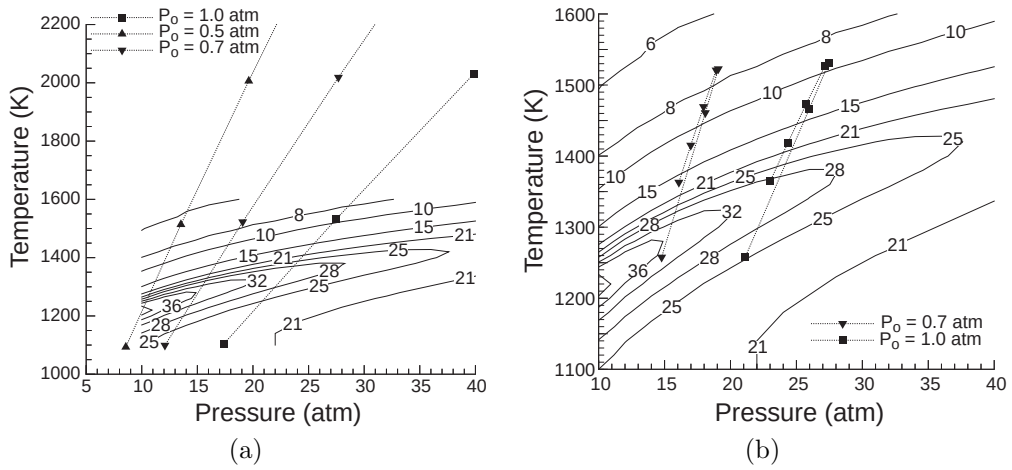

Figure 9: Post shock states for an oscillating detonation front superimposed on contours of θ for H_2-Air mixtures. The initial temperature for all simulations is 300 K and the initial pressure is varied according to the legend. (a) Stoichiometric mixtures corresponding to U/U_{CJ} of 0.8, 1.0, and 1.2 (from lowest to highest) (b) Varying equivalence ratios

In order to validate this model, constant volume explosion computations were performed and compared to the results of simulations with the detailed reaction mechanism. Figure 10a shows θ contours in the post-shock temperature-pressure plane. Solid lines were produced with the five-step model and dashed lines with stoichiometric H_2-O_2 with 85% argon dilution. As depicted in Fig. 10b, with appropriate rate constants, the current model exhibits the same extended limit (broken lines) as the detailed reaction mechanism. In this case, the extended second limit coincides with the ridge in θ. The maximum θ is located at where the value of the reaction rate for S3 is 1.3 to 1.5 times larger than that of S2, which is consistent with results from Oran and Boris (1982) and Shepherd (1986).

Figure 11 shows a superimposed contour plot for the ratio of τ to δ, in the temperature-pressure plane. Again, solid lines were produced with the five-step model and dashed lines with stoichiometric H_2-O_2 with 85% argon dilution simulations. The simplified model results match well with the detailed kinetics model results in the low pressure range. At higher temperatures and pressures, the difference increases but remains within a order of magnitude. The discrepancy is due to the fact that the reaction constants in the reduced model are validated with those of the detailed kinetics model at low pressures only.

In the future, we plan to use the five-step model to carry out multi-dimensional simulations of unsteady propagating detonations. We will examine the computed cellular structure for cases with von Neumann states located in various regions in the temperature-pressure plane particularly near the reduced effective activation energy ridge. When states within the reaction zone pass through the extended limit, we expect that the transition from one dominant mechanism to another will have a significant influence on the cellular structure.

It is interesting to contrast this model with the work of Eckett (2000), who developed a three-step model based on the quasi-steady state approximation following the ideas of Paczko and Klein (1993). That model also considered the competition for H atoms and Eckett found that it was essential to consider the evolution of HO_2 in order to reproduce the reaction structure over a reasonable range of compositions for hydrogen-air mixtures.. The species O, OH, and H_2O_2 were all taken to be in quasi-steady state, which resulted in a set of three algebraic constraints. The evolution of the remaining species, H, H_2, O_2, HO_2, and H_2O were solved by integrating the rate equations corresponding to the

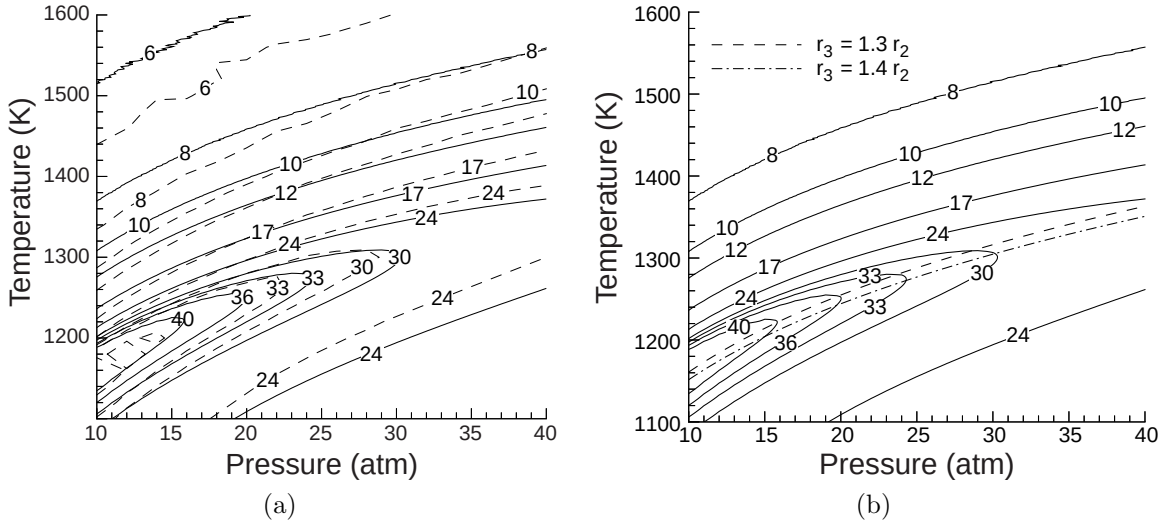

Figure 10: (a) Comparison of θ contours generated with the proposed five-step model and θ contours simulated using CV explosion calculations with detailed chemistry for stoichiometric H_2-O_2 with 85% argon dilution. (b) Classical extended second limit calculated with the model superimposed on contours of θ also generated by the model.

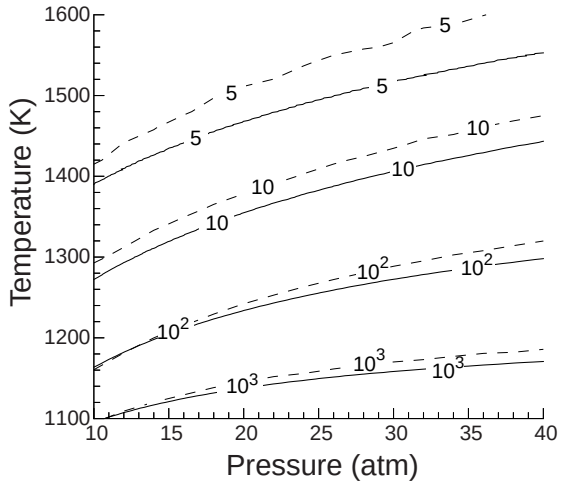

Figure 11: Comparison of τ/δ contours generated with the proposed five-step model and τ/δ contours simulated using CV explosion calculations with detailed chemistry for stoichiometric H_2-O_2 with 85% argon dilution.

following reduced mechanism

$$3H_2 + O_2 \rightleftharpoons 2H + 2H_2O, \tag{I}$$

$$2H \rightleftharpoons H_2, \tag{II}$$

$$HO_2 + H \rightleftharpoons H_2 + O_2. \tag{III}$$

Conservation of H and O atoms supplied the remaining two constraints. Although apparently simpler than the five-step model, the algebraic constraints in the QSSA model impose additional computational overhead. One-dimensional unsteady computations comparing the QSSA model with a detailed reaction

mechanism indicated that the QSSA model gave excellent results for the shape of the reaction zone although the reduced model under-predicted the reaction zone length by about 50%. For this reason, the stability limits and oscillation periods predicted by the QSSA model disagreed with the results of the detailed model. In the proposed five-step model, the rate constants can be adjusted to match the induction time so that better agreement with the detailed chemistry can be achieved.

5 Summary

We have examined the constant volume explosion reaction zone structure using detailed chemical kinetics for hydrogen, methane, and ethylene and conditions appropriate to fuel-oxygen-diluent detonation in laboratory or field experiments. Computations of induction time, energy release time, and effective activation energy for all three mixtures show that only in hydrogen does there appear to be a region of rapid change in reaction mechanism with changing thermodynamic conditions within the reaction zone.

In mixtures with hydrogen as fuel, the competition for H atoms produces a broad zone of high effective activation energy in the temperature-pressure plane. The peak of the activation energy appears coincident with the classical extended second limit as specified by reaction rate ratios. Although a change in reaction mechanism and effective activation energy is observed when crossing this zone, experimental measurements indicate detonations are possible above and below this zone. A "cross-over" temperature which is a function of pressure can be used to define the center of this zone, but it does not define a detonability limit or in any way indicate that chemical reaction will stop. This is in direct contradiction to the interpretation of the cross-over temperature in the three-step model. Examination of the results of simulations with detailed reaction mechanisms indicates that a realistic simplified model must include the subsequent reactions of the products of the termination reaction that competes with chain branching. We have proposed such a model and are in the process of exploring the implications for detonation modeling.

For mixtures with methane and ethane as fuel, simulations of near-stoichiometric mixtures with air shows no evidence of any sort of dramatic mechanism shift or cross-over effect for a wide range of temperature-pressure conditions. Apparently, a relatively simple reaction model of type proposed by Varatharajan et al. (2005) would be adequate in these cases since the induction and energy release times have a very smooth and simple dependence on the thermodynamic state. Since there is no cross-over effect of any type observed with these fuels, it is clear that the cross-over effect is not universal. In combination with our observations about the nature of the cross-over effect itself, we conclude that the cross-over effect and a cross-over temperature cannot be the basis for a theory of detonation limits or critical initiation energy.

The results of our simulations show that substantial variations in the ratio of induction time to energy release time occur as a function of post-shock temperature and pressure. The implication is that these are not universal parameters specific to a mixture but depend strongly on the initial conditions and oscillation of the leading shock front. Large values, on the order of 10^3, of the ratio τ/δ are possible for fuel-air mixtures, particularly at low temperatures characteristic of lean conditions. This is indicative of the computational difficulties that will be experienced in attempting direct simulation of multidimensional unsteady detonations with any sort of reaction modeling.

We have proposed that as minimum requirements, any realistic simplified reaction mechanism must match the induction time, energy release time, and reduced effective energy dependence on temperature and pressure behind an unstable shock front. However, this is simply a minimum requirement and it may be necessary to do far more in some situations. All of our considerations in this paper are based on a very simplified steady model of the chemical processes within detonations. While this may be adequate for weakly unstable detonation waves and slow transients, there are many situations where this may not apply. For example, it is known that unsteady effects can be quite significant in initiation (Eckett et al., 2000), diffraction (Arienti and Shepherd, 2005a), and it may be necessary to consider diffusive transport (Arienti and Shepherd, 2005b) in modeling the propagation of highly unstable waves (Radulescu et al., 2005). In all of these cases, the detailed behavior of the radical pool may play an essential role, and

development of a simplified mechanism appears to be much more challenging.

Acknowledgments

Z. Liang is supported by a Fellowship from NSERC, Canada and S. Browne is supported by an NSF Graduate Fellowship. We thank D. Goodwin for writing and supporting Cantera.

References

M. Arienti and J. E. Shepherd. A numerical study of detonation diffraction. *J. Fluid Mech.*, 529:117–146, 2005a. 15

M. Arienti and J. E. Shepherd. The role of diffusion in irregular detonations. The 4th Joint Meeting of the US Sections of the Combustion Institute, Philadelphia, PA, March 20-23, 2005b. 15

J. M. Austin, F. Pintgen, and J. E. Shepherd. Reaction zones in highly unstable detonations. In *Proceedings of the Combustion Institute*, volume 30, pages 1849–1857, 2005. 4

F. E. Belles. Detonability and chemical kinetics: Predictions of limits of detonability of hydrogen. In *Seventh Symposium (International) on Combustion*, pages 745–751, 1959. 2

A. A. Borisov. On the origin of exothermic centers in gaseous mixtures. *Acta Astronautica*, 1:909–920, 1974. 3

S. Browne and J. E. Shepherd. Numerical solution methods for control volume explosions and znd detonation structure. URL http://www.galcit.caltech.edu/~stbrowne/SD_toolbox/matlab.html. 2005. 4

J. W. Dold and A. K. Kapila. Comparison between shock initiations of detonation using thermally-sensitive and chain-branching chemical models. *Combustion and Flame*, 85:185–194, 1991. 2

S. B. Dorofeev, V. P. Sidorov, M. S. Kuznetsov, I. D. Matsukov, and V. I. Alekseev. Effect of scale on the onset of detonations. *Shock Waves*, 10(2):137–149, May 2000. 2

J. E. Dove and T. D. Tribbeck. Computational study of the kinetics of the hydrogen-oxygen reaction behind steady state shock waves. application to the composition limits and transverse stability of gaseous detonations. *Astronautica Acta*, 15:387–397, 1970. 2

C. A. Eckett. *Numerical and Analytical Studies of the Dynamics of Gaseous Detonations*. PhD thesis, California Institute of Technology, Pasadena, California, September 2000. 1, 13

C. A. Eckett, J. J. Quirk, , and J. E. Shepherd. The role of unsteadiness in direct initiation of gaseous detonations. *Journal of Fluid Mechanics*, 421:147–183, 2000. 15

W. Fickett and W. Davis. *Detonation*. Dover Publications, 1979. 1, 4

W. D. Fickett, J. D. Jacobson, and G. L. Schott. Calculated pulsating one-dimensional detonations with induction zone kinetics. *AIAA Journal*, 10:514–516, 1972. 3

W. C. Gardiner and C. B. Wakefield. Influence of gasdynamic processes on the chemical kinetics of the hydrogen-oxygen explosion at tempeartures near 1000 k and pressures of several atmospheres. *Astronautica Acta*, 15:399–409, 1970. 3

D. Goodwin. Cantera: Object-oriented software for reacting flows. Technical report, California Institute of Technology, 2005. URL http://www.cantera.org. 4

B. F. Gray and C. H. Yang. On the unification of the thermal and chain theories of explosion limits. *Journal of Physical Chemistry*, 69(8):2747–2750, 1965. 2

GRI. Gri-mechanism 3.0. URL http://www.me.berkeley.edu/gri_mech. 4, 6, 8

J. H. Lee. Dynamic parameters of gaseous detonations. *Annu. Rev. Fluid Mech.*, 16:311–336, 1984. 2

B. Lewis and G. von Elbe. *Combustion, Flame and Explosions of Gases*. Academic Press, 2nd edition, 1961. 2

Z. Liang and L. Bauwens. Cell structure and stability of detonations with a pressure dependent chain-branching reaction rate model. *Combust. Theory Model.*, 9:93–112, 2005. 1, 2

T. F. Lu, C. K. Law, and Y. G. Ju. Some aspects of chemical kinetics in chapman-jouguet detonation: Induction length analysis. *Journal of Propulsion and Power*, 19(5):901–907, 2003. 1

J. W. Meyer and A. K. Oppenheim. On the shock-induced ignition of explosive gases. In *Proceedings of the Thirteenth Symposium (International) on Combustion*, pages 1153–1164, 1970. 3

J. W. Meyer and A. K. Oppenheim. Coherence theory of the strong ignition limit. *Combustion and Flame*, 17:65–68, 1971. 3

H. D. Ng, Yiguang Ju, and John H. S. Lee. Study of detonation sensitivity of hydrogen-air mixture using an updated comprehensive chemical kinetic mechanism. 20th ICDERS, Montreal, CA, 2005. 3, 5

H. D. Ng and J. H. S. Lee. Direct initiation of detonation with a multi-step reaction scheme. *Journal of Fluid Mechanics*, 476:179–211, 2003. 2, 3

E. S. Oran and J. P. Boris. Weak and strong ignition. II. Sensitivity of the hydrogen-oxygen system. *Combustion and Flame*, 48:135–148, 1982. 3, 13

G. Paczko and R. Klein. Reduced chemical kinetic schemes for hydrogen–air–steam detonation simulations. Unpublished. Presented at *14th ICDERS*, Coimbra, Portugal, 1993. 13

F. Pintgen and J. E. Shepherd. Pulse detonation engine impulse analysis for partially-oxidized jet fuel. GALCIT Report FM2003.001, 2003. 5

M. I. Radulescu, G. J. Sharpe, J.H.S. Lee, C.B. Kiyanda, A. J. Higgins, and R. K. Hanson. The ignition mechanism in irregular structure gaseous detonations. In *Proceedings of the Combustion Institute*, volume 30, pages 1859–1867, 2005. 15

E. Schultz and J. E. Shepherd. Validation of detailed reaction mechanisms for detonation simulation. Technical Report FM99-5, GALCIT, 2000. 5

N. N. Semenov. *Chemical Kinetics and Chain Reactions*. Clarendon Press, Oxford, 1935. 2

J. E. Shepherd. Chemical kinetics of hydrogen–air–diluent detonations. *PAA*, 106:263–293, 1986. 2, 13

M. Short and J. J. Quirk. On the nonlinear stability and detonability limit of a detonation wave for a model three-step chain branching reaction. *Journal of Fluid Mechanics*, 339:89–119, 1997. 1, 2, 3

M. Short and G. J Sharpe. Pulsating instability of detonations with a two-step chain-branching reaction model: theory and numerics. *Combustion Theory and Modelling*, 7(2):401–416, 2003. URL http://stacks.iop.org/1364-7830/7/401. 3

R. A. Strehlow and A. Cohen. Initiation of detonation. *Physics of Fluids*, 5(1):97–101, 1962. 2

R. A. Strehlow and C. D. Engel. Transverse waves in detonation II. structure and spacing in h_2-o_2, c_2h_2-o_2, c_2h_4-o_2 and ch_4-o_2 systems. *AIAA Journal*, 7:492–496, 1969. 3

S. R. Tieszen, M. P. Sherman, W. B. Benedick, J. E. Shepherd, R. Knystautas, and J. H. S. Lee. Detonation cell size measurements in hydrogen-air-steam mixtures. In *Prog. Astronaut. Aeronaut.*, volume 106, pages 205–219, 1986. 2, 8

B. Varatharajan, M. Petrova, F. A. Williams, and V. Tangirala. Two-step chemical-kinetic description for hydrocarbon-oxygen-diluent ignition and detonation applications. In *Proceedings of the Combustion Institute*, volume 30, pages 1869–1877, 2005. 1, 15

B. Varatharajan and F. A. Williams. Chemical-kinetic descriptions of high-temperature ignition and detonation of acetylene-oxygen-diluent systems. *Combustion and Flame*, 124(4):623–645, 2001. 1

B. Varatharajan and F. A. Williams. Ethylene ignition and detonation chemistry, part 1: Detailed modeling and experimental comparison. *Journal of Propulsion and Power*, 18(2):344–351, 2002a. 1

B. Varatharajan and F. A. Williams. Ethylene ignition and detonation chemistry, part 2: Ignition histories and reduced mechanisms. *Journal of Propulsion and Power*, 18(2):352–362, 2002b. 1

V. V. Voevodesky and R. I. Soloukhin. On the mechanism and explosion limits of hydrogen-oxygen chain self-ignition in shock waves. In *Proceedings of the Tenth Symposium (International) on Combustion*, pages 279–283, 1965. 2, 3, 9

S. Yungster and K. Radhakrishnan. Pulsating one-dimensional detonations in hydrogen–air mixtures. *Combustion Theory and Modelling*, 8(4):745–770, 2004. URL http://stacks.iop.org/1364-7830/8/745. 3

S. Yungster and K. Radhakrishnan. Structure and stability of one-dimensional detonations in ethylene-air mixtures. *Shock Waves*, 2005. DOI: 10.1007/s00193-005-0242-0. 3